JOURNAL OF MATERIALS SCIENCE 33 (1998) 3275–3284

Effect of secondary-phase segregation on the positive temperature coefficient in resistance characteristics of n-$BaTiO_3$ ceramics

N. S. HARI, T. R. N. KUTTY
Materials Research Centre, Indian Institute of Science, Bangalore 560 012, India
E-mail: kutty@mrc.iisc.ernet.in

Modifications in the positive temperature coefficient in resistance (PTCR) of n-$BaTiO_3$ ceramics are brought about by specific additives such as Al_2O_3, B_2O_3 or SiO_2, leading to the segregation of secondary phases such as $BaAl_6TiO_{12}$, BaB_6TiO_{12} or $BaTiSi_3O_9$ at the grain boundaries. Segregation of barium aluminotitanates resulted in broad PTCR curves, whereas B_2O_3 addition gave rise to steeper jumps and SiO_2 addition did not result in much broadening compared with donor-only doped samples. Microstructural studies clearly show the formation of a structurally coherent epitaxial second phase layer of barium aluminotitanate surrounding the $BaTiO_3$ grains. Electron paramagnetic resonance investigations indicated barium vacancies, V_{Ba}, as the major electron trap centres which are activated across the tetragonal-to-cubic phase transition according to the process $V_{Ba}^{X} + e' \rightleftharpoons V_{Ba}'$. The grain size dependence of the intensity of the V_{Ba}' signal indicated the concentration of these trap centers in the grain-boundary layer (GBL) regions. Further, the charge occupancy of these centres is modified by the secondary phases formed through grain-boundary segregation layers. $BaAl_6TiO_{12}$ gave rise to Al-O^- hole centres whereas no paramagnetic centres corresponding to boron could be detected on B_2O_3 addition. Such secondary phases, forming epitaxial layers over the $BaTiO_3$ grains, modify the GBL region, rich in electron traps, surrounding the grain core. The complex impedance analyses support this three-layer structure, showing the corresponding contributions to the total resistance which can be assigned as R_g, R_{gb} and $R_{\text{secondary phase}}$. The epitaxial second phase layers bring about inhomogeneity in the spatial distribution of acceptor states between the grain boundary and the grain bulk resulting in extended diffuse phase transition characteristics for the GBL regions in n-$BaTiO_3$ ceramics. This can cause the GBL regions to have different transition temperatures from the grain bulk and a spread in energy levels of the associated GBL trap states, thus modifying the PTCR curves. An attempt has been made to explain the results based on the vibronic interactions applied to the mid-band-gap states in n-$BaTiO_3$.

1. Introduction

In semiconducting polycrystalline ceramics, the bulk characteristics are intricately related to the composition and structure of grains as well as grain boundaries. The electrical behaviour of the boundaries is associated with the charge-transfer process. The segregated impurities, the precipitated second phase and the distribution of the frozen-in point defects at the grain boundaries play major roles in determining the overall electrical properties. The well-known grain-boundary phenomenon in donor-doped semiconducting $BaTiO_3$, namely the positive temperature coefficient in resistance (PTCR), has been attributed to the formation of electrical barriers at the grain boundaries across the tetragonal-to-cubic phase transition [1]. These barriers are reported to arise from acceptor states near the grain boundary which trap electrons. A more recent review by Huybrechts *et al.* [2] showed that the PTCR effect cannot be explained by assuming only one kind of electron trap. Native defects such as barium vacancies, V_{Ba}, titanium vacancies, V_{Ti}, adsorbed gases at the grain boundaries, or 3d transition-metal ion impurities can act as electron traps, with experimental evidence supporting one or the other [3–16]. This has kindled renewed interest in the subject of PTCR. The differential distribution of these electron traps as well as the formation of new electron traps by the alien constituents segregating at the grain boundaries can significantly alter the PTCR in $BaTiO_3$. Segregation studies on $BaTiO_3$ have been made previously by Lewis *et al.* [6]. From calculations of the bulk and surface defect energies, they proposed that there is a strong tendency for segregation of acceptor states in low-charge states. Also, the activation energy for the migration of acceptors in the titanium sublattice is very high and hence donors will deplete the

grain-boundary area, leaving behind an acceptor-rich layer, which leads to n–i–n junctions responsible for the PTCR effect. However, according to the segregation studies made by Chiang and Takagi [15], the spatial distribution of the acceptor defects at the grain boundary can be neglected compared with the electron depletion layer width. Therefore the acceptor layer caused by segregation is assumed to be one dimensional in the Heywang [1] model, but the acceptor levels in the samples of Chiang and Takagi [15] were much higher (0.3–1.0 mol%) than PTCR doping levels. Through similar segregation studies, Desu and Payne [16] proposed an n–i–n model; contrary to the calculations of Lewis *et al.* [6], the donors are said to be segregated at the grain boundaries, creating an insulating layer through vacancy compensation and forming the grain-boundary barriers. Again, the donor (10 mol% Nb) and the acceptor levels (0.6 at% Fe) used by them were much higher than the PTCR doping levels, namely 0.1–0.3 at% donor and 0.01–0.05 at% acceptor, and hence the model is questionable *vis-à-vis* the PTCR effect. Further, the experimental techniques used by them (scanning Auger electron spectrosocopy and scanning transmission electron microscopy) yielded results which were specific to a few grains or grain boundaries and were not the average over all the grains or grain boundaries in the specimen. Experimental evidence exists in the literature [17–19], by way of electron paramagnetic resonance (EPR) measurements on single crystals and polycrystalline $BaTiO_3$ ceramics, to show that the acceptors do not segregate at the grain boundaries but dissolve within the grain bulk at the concentration levels used for PTCR. Both single crystals and polycrystals showed the same set of EPR signals arising from the acceptor ions (mostly 3d transition-metal ions). Apart from the bulk dopants, segregation of grain-boundary modifiers such as Al_2O_3, SiO_2 and TiO_2 in $BaTiO_3$ polycrystalline ceramics, owing to limited solid solubility, is known [13, 20–26]. They form segregated layers at grain boundaries and also randomly distributed secondary phases when present in higher concentrations (greater than 1 mol%). These have been used as aids to lower the sintering temperature but their effect on the PTCR of $BaTiO_3$ has not been dealt with in detail. No reports exist on the possible formation of aluminotitanates or silicotitanates of barium along the grain boundaries, nor on the polytitanates of barium. These secondary phases can modify the distribution of grain-boundary electron traps, thus directly influencing the electrical characteristics of n-$BaTiO_3$ ceramics. Unlike acceptor dopants, these segregated species can have a higher tolerance limit (up to a few per cent) of addition without increasing the room-temperature resistivity. Furthermore, no report exists on the difference in behaviour when these modifiers are bulk doped in raw material $BaTiO_3$ powder, in comparison with the heterogeneous addition during the ceramic fabrication. In view of the lack of detailed studies on the segregation effects of grain-boundary modifiers on PTCR of $BaTiO_3$ and to understand the role of these in modifying the grain-boundary electrical barriers, we have investigated the changing effects in PTCR brought about by specific grain-boundary modifiers such as Al_2O_3, B_2O_3 or SiO_2 in donor-doped $BaTiO_3$. The resulting grain-boundary segregation or second-phase formation can affect the electrical conduction possibly through the formation of new types of defect state and their differential distribution between grain boundary and grain bulk. EPR spectroscopy has been used as a tool, as in the previous studies by our group [17, 18, 27], for investigating the grain-boundary trap states in donor-doped $BaTiO_3$. Impedance spectroscopy studies were carried out to monitor the contributory components from the grain-boundary layers (GBLs), leading to an explanation for the drastic change in PTCR with different grain-boundary modifiers.

2. Experimental procedures

Preparation of fine powders and the processing of ceramics have been described elsewhere [17, 28, 29]. The starting material was obtained by the thermal decomposition of $BaTiO(C_2O_4)_2 \cdot 4H_2O$ (BTO). In order to observe the changing pattern of trap centres associated with native defects by EPR, the $BaCl_2$ to $TiOCl_2$ ratio was varied from 0.9 to 1.1 following the method adopted in [17, 30]. Although the resulting $BaTiO_3$ has a correspondingly small deviation in stoichiometry leading to possible enhancement in V_{Ba} X-ray powder diffractogram showed phase singularity. The background impurities in the starting material were kept as low as possible (Mn, less than 0.1 $\mu g\, g^{-1}$; Fe, less than 1$\mu g\ g^{-1}$) by the procedure described in [17]. Nb (0.2–0.4 at%, i.e., $(3.1–6.3) \times 10^{19}$ ions cm^{-3}) was used as the donor and separately, Mn (25–200 ppm, i.e., $(0.16–1.17) \times 10^{19}$ ions cm^{-3}) was used as the acceptor. Donor concentrations greater than 0.4 at% resulted in smaller grain sizes. The grain boundary modifiers (Al_2O_3, B_2O_3 or SiO_2) were added heterogeneously, i.e., by mixing the preheated donor doped $BaTiO_3$ powder with the modifier and pressing into green discs. The addition of Al_2O_3 resulted in the formation of secondary phases such as $BaAl_6TiO_{12}$ and $Ba_3Al_{10}TiO_{20}$ along the grain boundaries. B_2O_3 addition did result in the formation of distinct secondary phase but was not detectable by X-ray diffraction. It is possible that B_2O_3 can form a glassy phase having the composition BaB_6TiO_{12}. SiO_2 led to the formation of second phases such as $BaTiSi_3O_9$ (benitoite).

The powder mixtures were mixed with an organic binder and pressed at 200 MPa to obtain green ceramics of 65–70% compaction. The binder was subsequently burnt off at 1100 K in air. The discs were then sintered in static air at 1650 K to obtain ceramics of 1–25 μm grain size. The sinter density of the ceramic discs ranged from 92 to 97% of the single-crystal value. Ceramics of different grain sizes were obtained by varying the sintering conditions for a given composition or by increasing the donor concentration to more than 0.4 at%. The ceramic discs were polished after sintering so that layers of 20–30 μm on both the sides were removed, in order to ensure that the measured characteristics did not correspond to those of

external surface regions. Ohmic metal contacts were then made by electroless nickel plating [31].

The ρ–T measurements were carried out at low-voltage signals (less than 0.5 V) while the sample temperature was varied from 298 to 700 K at a constant rate of 2 K min^{-1}. Microstructural studies of polished and etched or fractured discs were carried out using a S360 Cambridge scanning electron microscope with an ultimate resolution of 4 nm. This instrument was fitted with fully automated equipment for quantitative energy-dispersive X-ray analysis (EDXA). EPR spectra were recorded using a Varian E109 X-band spectrometer having a TE_{011} cavity, in the temperature range from 80 to 550 K. For ready comparison of intensities, the amounts of sample (150 mg), microwave powers and modulation amplitudes were kept the same. The EPR signal intensities were expressed as double integrated intensities (DIIs) calculated from the empirical relation [32]

$$\mathrm{DII} = \frac{(\text{signal height})(\text{signal width})^2}{(\text{gain})(\text{sample mass})(\text{modulation amplitude})(\text{power})^{1/2}} \quad (1)$$

Measurements of the impedance, Z, were carried out using an HP4194A impedance–gain phase analyser at a signal strength of 0.5 V_{rms}.

3. Results

3.1. Resistivity–temperature (ρ–T) characteristics

Fig. 1 shows the PTCR characteristics of donor-doped $BaTiO_3$ with different grain boundary modifiers. The PTCR jump may be defined as the magnitude of the difference between ρ_{max} and ρ_{min}. Ceramics containing donor alone show a PTCR jump of about six orders of magnitude whereas, for the ceramics formulated with Al_2O_3 as the grain-boundary modifier, the PTCR jumps are quite broad with decreased ρ_{max}, but the room-temperature resistivity is decreased. T_{max} is as high as 600 K with 3 mol% Al_2O_3 (Fig. 1). The scanning electron micrographs (Fig. 2) show the presence of secondary phases along the grain boundary and triple junctions. For more than 2 mol% Al_2O_3, a thin platy second phase, clearly distinguishable from the nearly rounded grains, is observed which appears as needle shaped from the side of the fractured surfaces (Fig. 2a). These are identified as $BaAl_6TiO_{12}$ from EDXA [33]. The presence of rounded grains and the solidification bands suggest the influence of a liquid phase (Fig. 2b) during sintering. The scanning electron micrographs clearly show the uniform coating of the secondary phases surrounding the $BaTiO_3$ grain, which can form a structurally coherent epitaxial layer. For the ceramics containing B_2O_3, the PTCR is much steeper as a result of the shift in T_{max} to as low as 420 K for 1 mol% B_2O_3 or less (Fig. 1). However, the magnitude of the PTCR jump remains nearly the same as that of the specimens without B_2O_3 with comparable ρ_{max}. The ρ_{RT} increases with increasing B_2O_3 concentration and above 2 mol% the ceramics become highly resistive. The addition of SiO_2 does not result in much broadening of the PTCR jump (Fig. 1). Silica forms distinctly identifiable secondary phases, such as $BaTiSi_3O_9$, along grain boundaries and triple junctions which, in turn, does not form solid solutions with

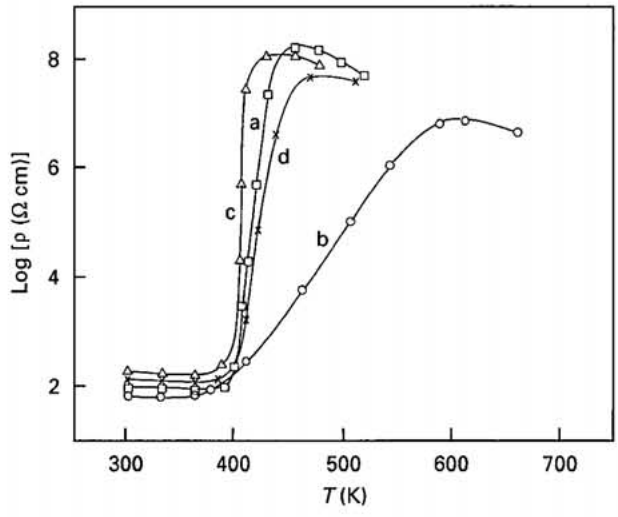

Figure 1 ρ–*T* characteristics of $BaTiO_3$ + 0.3 at% Nb with no grain-boundary modifier (curve a), 3 mol% Al_2O_3 (curve b), 1 mol% B_2O_3 (curve c) and 3 mol% SiO_2 (curve d).

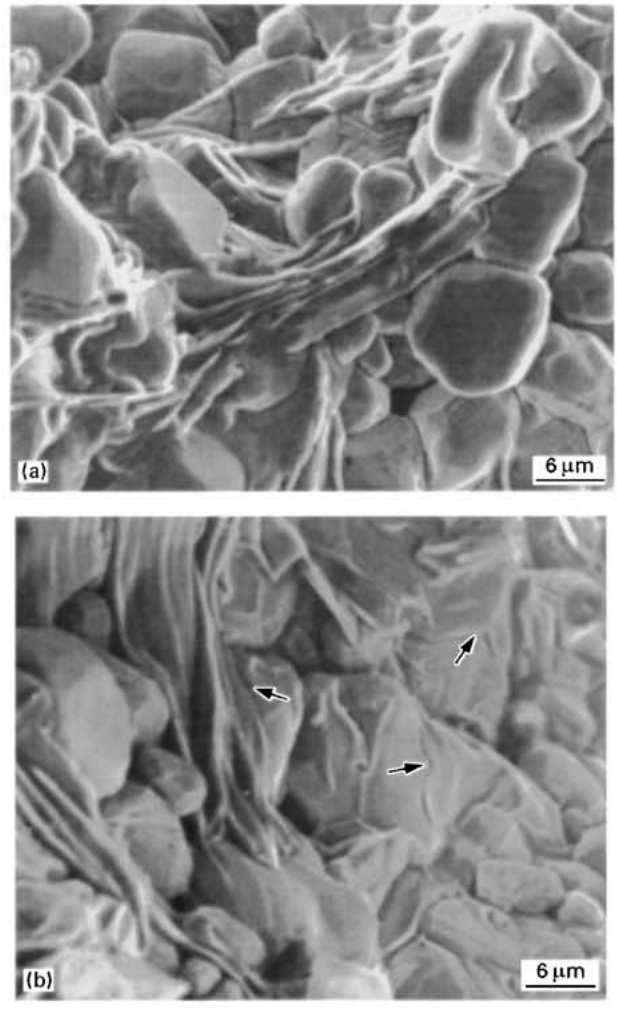

Figure 2 Microstructure of $BaTiO_3$ + 0.3 at% Nb + 3 mol% Al_2O_3. The coherence of the secondary phases by way of over growth on $BaTiO_3$ grains is shown by the arrows in (b).

$BaTiO_3$. Broadening of the ρ–T characteristics indicates enhanced disorder at the GBLs through the formation of secondary phases which can induce modifications in the spatial distribution of point defects with respect to grain core or grain-boundary regions.

3.2. Electron paramagnetic resonance

EPR studies have been carried out to observe the changing pattern of trap states. The undoped $BaTiO_3$ did not show any EPR signals, indicating the absence of any paramagnetic impurities above the detection limits of EPR spectroscopy. Fig. 3 shows the EPR signals for $BaTiO_3$ + 0.3 at% Nb exhibiting PTCR at temperatures corresponding to the stability regions of the four crystallographic modifications. At room temperature, $BaTiO_3$ + 0.3 at% Nb showed an asymmetric signal with $g = 1.963$ and a very weak signal having $g = 1.997$ (Fig. 3). Above T_g the $g = 1.963$ signal becomes symmetric together with a pronounced gain in intensity for the $g = 1.997$ signal. The variation in DII of the $g = 1.997$ signal with temperature (Fig. 3) shows the pronounced intensity of this signal in the rhombohedral and cubic phases.

EPR signals with $g = 1.963$ and $g = 1.997$ have been reported earlier [17, 27] for donor-doped as well as H_2-reduced $BaTiO_3$ ceramics. Since the intensity of the $g = 1.963$ signal increased with increasing degree of reduction together with increased conductivity, it was reported to arise from shallow donor-type centres, possibly trapped electrons, resonating between the oxygen vacancy and two of the adjoining titanium ions (Ti^{3+}–V_o–Ti^{4+} defect centres). This model is also in agreement with the oxygen loss observed by mass spectrometry by Drofenik *et al.* [34] and the mass loss studies in semiconducting $BaTiO_3$ [35]. From the appearance of the $g = 1.997$ signal above T_c and its increase in intensity with decreased [Ba]/[Ti] values in the precursor oxalate even for the undoped H_2-reduced samples [17, 27], it was concluded that this signal originated from barium vacancies, which should be from the singly ionized centres, V'_{Ba}, since the spin pairing in doubly ionized defect centres, V''_{Ba}, makes them EPR inactive. Considering the very low concentration of V''_{Ba} in the temperature region of the PTCR, shown from the defect chemistry studies [36], and the increase in resistivity above the Curie point, the conversion $V^{X}_{Ba} + e' \rightleftharpoons V'_{Ba}$ was suggested across the phase transition to explain PTCR, the barium vacancies existing as neutral entities in the tetragonal phase.

The present results show that the intensity of $g = 1.997$ signal in the cubic phase also depends on the donor concentration (Fig. 4), their intensity now being much higher compared with that of the undoped H_2-reduced $BaTiO_3$ samples. Also the DII of $g = 1.997$ is maximum in the absence of grain-boundary segregated impurities. The appearance of this signal must be due to the changes in the crystal symmetry rather than the absence of spontaneous polarization, P_s, since the signal is present in the orthorhombic and rhombohedral phases of $BaTiO_3$ which are ferroelectric. The intensity of $g = 1.997$ also shows an inverse relation to the average grain size of the ceramics; the latter can be varied by changing the sintering parameters for a given composition of doped $BaTiO_3$. That the $g = 1.963$ and $g = 1.997$ signals do not arise from the $|+\frac{1}{2}\rangle \leftrightarrow |-\frac{1}{2}\rangle$ transition of background Cr^{3+} and Fe^{3+} impurities, respectively, is confirmed by the intentional doping of these acceptor ions. The $g \approx 2.00$ signal of Fe^{3+} [37, 38] and the $g = 1.961$

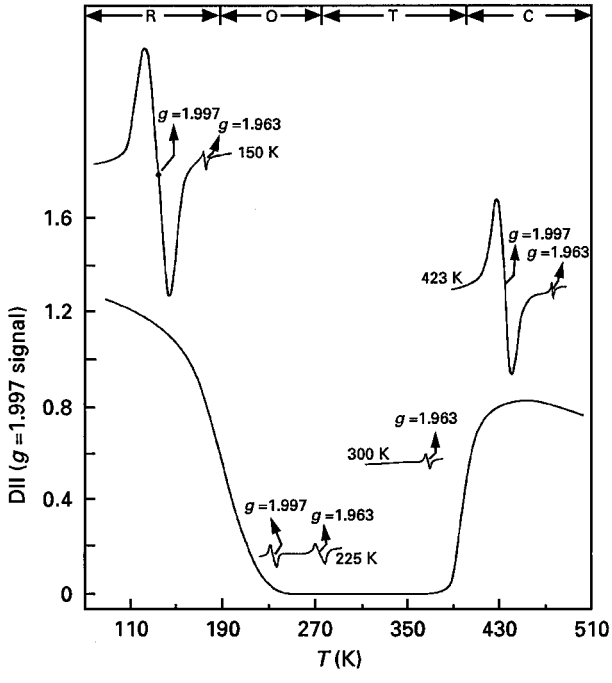

Figure 3 Variation in DII of the $g = 1.997$ signal with temperature for $BaTiO_3$ + 0.3 at% Nb. The EPR signals ($g = 1.963$ and $g = 1.997$) of the sample in all the four phase stability regions is also shown. For direct comparison of the signals, the receiver gain of the EPR spectrometer was kept constant. C, cubic; T, tetragonal; O, orthorhombic; R, rhombohedral.

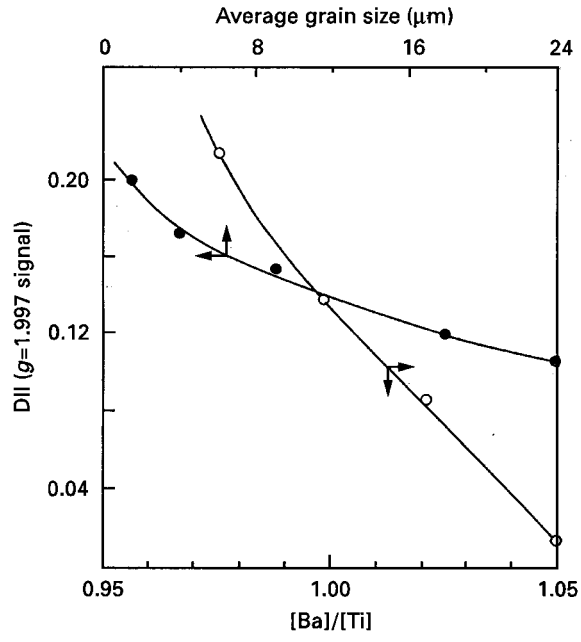

Figure 4 Variation in DII of the $g = 1.997$ signal for $BaTiO_3$ + 0.3 at% Nb with [Ba]/[Ti] ratio (○) at 423 K, and average grain size (●) at 300 K.

signal of Cr^{3+} [39] did not show any discernible variation across the tetragonal-to-cubic phase transition temperature.

Fig. 5 shows the EPR spectra of PTCR $BaTiO_3$ + 0.3 at% Nb containing 25 ppm Mn acceptor as well as Al_2O_3 as grain-boundary modifier additive. No signal arising from Mn is observable at 300 K. In fact, the specimen is identical with that of $BaTiO_3$ + 0.3 at% Nb and shows a similar variation in EPR spectra with temperature. Above 400 K (in the paraelectric cubic phase), the six-line signal having the hyperfine splitting parameters corresponding to Mn^{2+} signal appears. These six lines were misinterpreted, at first, as arising from the hyperfine components of titanium ion (^{49}Ti isotope of about 7% abundance) [37], but were later identified to arise from $|+\frac{1}{2}m_I\rangle \leftrightarrow |-\frac{1}{2}m_I\rangle$ transition of Mn^{2+} impurities occupying the Ti^{4+} sites [40, 41]. The appearance of Mn^{2+} signals above T_c has been explained by the lattice symmetry dependent $Mn^{3+} + e' \rightleftharpoons Mn^{2+}$ conversion [18] arising from the relative shift of Mn^{3+} energy level towards the valence-band edge during the phase transformation. Mn exists as Mn^{3+} in the tetragonal phases which, owing to the very short relaxation time, is not observable by EPR at these temperatures. Thus Mn^{3+} acts as a trap centre for charge carriers. This effect auguments the trapping action of V_{Ba}^{X} to convert itself to V'_{Ba} across the tetragonal-to-cubic phase transition. Similar to V'_{Ba} the appearance of Mn^{2+} was also shown to be crystal structure dependent owing to the presence of this signal in other ferroelectric phases (less than 190 K) [18]. Although [Mn] is only one fifth to one twentieth of the donor concentration, [D], the number of Mn ions per cubic centimetre is still large, which will account for the criticism raised by Huybrechts *et al.* [2] regarding the effect of Mn in augumenting the charge carrier trapping by V_{Ba}^{X} across the phase transition to explain the significant increase in PTCR jump. It has been demonstrated earlier [42] that the variations in intensities of acceptor signals with temperature (e.g., Mn^{2+}) have an activation energy of the order of transverse optical (TO) phonon modes indicating the involvement of vibronic mechanism (interaction of lattice vibrations with the electronic states either from intrinsic defects or extrinsic impurities).

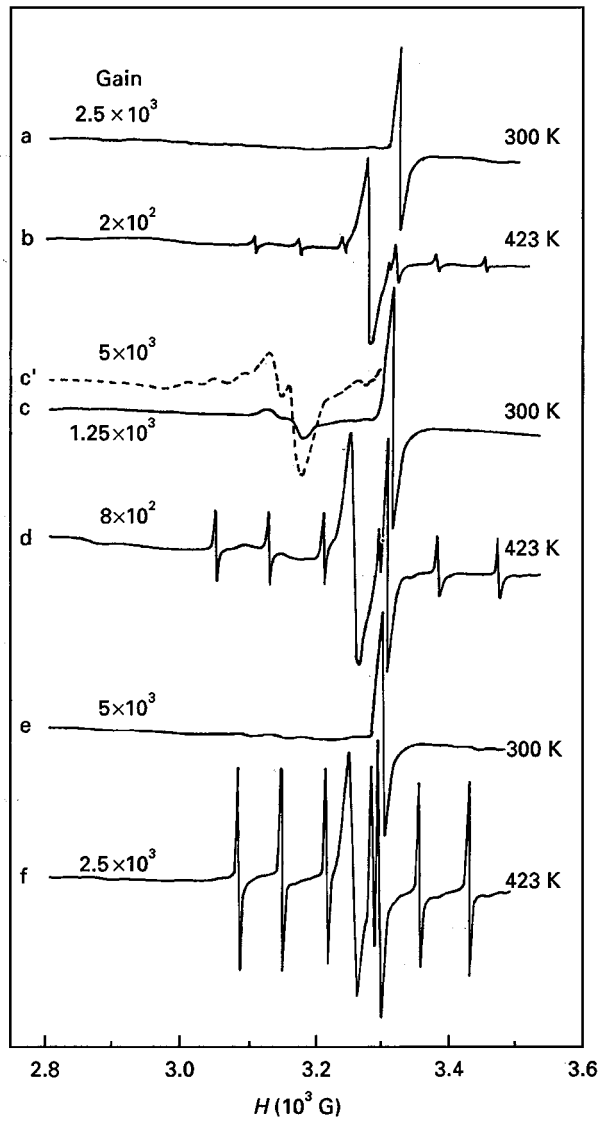

Figure 5 EPR spectra of $BaTiO_3$ + 0.3 at% Nb + 25 ppm Mn with no grain-boundary modifier (curves a and b), 3 mol% Al_2O_3 (curves c, c', and d), 1 mol% B_2O_3 (curves e and f).

The EPR spectra of the specimens formulated with Al_2O_3 showed two other asymmetric overlapping signals at 300 K with $g = 2.0537$ and $g = 2.0721$, as well as the $g = 1.963$ signal. These signals should arise from a hole centre because $\Delta g = g_{obs} - g_e$ is positive ($g_e = 2.0036$, which corresponds to a free electron). The increase in DII of the hole centres with decreasing grain size is explainable in terms of the enhanced concentration of these centres at the GBL regions. These hole centre signals are identified to originate from $Al\text{–}O^-$ defect centres [33]. The DII of these signals decreased with increasing temperature except for a peak around the Curie point (Fig. 5). The $g = 1.997$ signal appeared above T_c, but now with diminished intensity, reduced by about 2.5 times that of the specimens containing donor alone (Fig. 6).

For the specimens formulated with B_2O_3 as the grain-boundary modifier, no paramagnetic centres

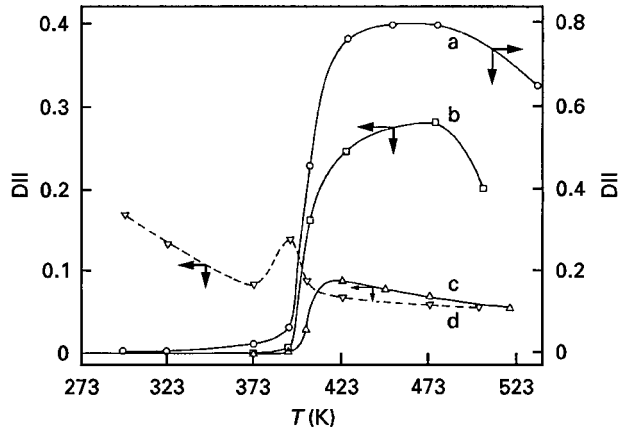

Figure 6 Variation in DII of the $g = 1.997$ signal in $BaTiO_3$ containing 0.3 at% Nb (curve a), 0.3 at% Nb + 3 mol% Al_2O_3 (curve b), 0.3 at% Nb + 1 mol% B_2O_3 (curve c). Curve d shows the variation in the hole centre in a specimen containing 0.3 at% Nb + 3 mol% Al_2O_3.

involving boron are observed. This can be due to the strong spin–lattice relaxation of boron impurity-related centres and the least stability for BO_6 in preference to BO_4 or BO_3 polyhedra. Accordingly, B_2O_3 may segregate to form a secondary glassy phase. Similar to donor-only samples, only one asymmetric signal with $g = 1.963$ is observed at 300 K and, above T_c, this becomes symmetric and the $g = 1.997$ signals appears. The change in intensity of $g = 1.997$ signal (Fig. 6) was nearly eight times lower than that of specimens with donor alone. This shows the effect of boron in suppressing the $g = 1.997$ signal above T_c.

Since PTCR is a grain-boundary phenomenon, the trap centres responsible for charge trapping across phase transition should be concentrated at the grain boundaries. In order to verify this, the EPR spectra of n-$BaTiO_3$ was studied as a function of grain size. Fig. 4 shows that the DII of the $g = 1.997$ signal decreases with increasing grain size (i.e., decreasing GBL), thus confirming that the defect centre giving rise to this signal should be concentrated more at the grain boundaries than in the bulk. This is also true for the Al–O^- hole centres present in ceramics formulated using Al_2O_3 as the grain-boundary modifier.

3.3. Complex impedance results

The complex impedance spectra of the specimens formulated with Al_2O_3 were studied above and below T_c to decipher the number of electrical components with which the grains and GBLs in $BaTiO_3$ ceramics are made up of. A detailed investigation of the complex impedance analysis of PTCR $BaTiO_3$ ceramics can be found in our earlier publications [43, 47]. Fig. 7 shows the results for 3 mol% Al_2O_3. Clearly, two semicircles and hence three contributary components to the total impedance could be deciphered. Since $BaAl_6TiO_{12}$ can segeregate at the grain boundaries, the three contributions can be attributed to the grain interior resistance (R_g), the grain-boundary resistance (R_{gb}) and that from the secondary phase ($R_{\text{secondary phase}}$). Such a three-component contribution is supported by the scanning electron microscopy (SEM) results which showed that the secondary phases form a coherent epitaxial layer surrounding $BaTiO_3$ grains. Also, the presence of three electrical components (namely the non-ferroelectric grain-boundary region, the ferroelectric shell-type outer grain region and the conductive grain cores) was indicated by Sinclair and West [44] in their complex impedance studies on n-$BaTiO_3$ ceramics. The low-frequency value of Z' (real part of the impedance), which is dominated by the grain-boundary resistance, increases to very high values above T_c resulting in a large area under the semicircle of the Cole–Cole plot. The variations in R_g and R_{gb} with temperature for the ceramics with and without grain-boundary modifiers are shown in Fig. 8. R_{gb} versus T shows exactly similar behaviour to that of the PTCR effect in bulk specimens. This confirms that Al_2O_3 indeed helps in the grain-boundary segregation of $BaAl_6TiO_{12}$, thereby increasing the density of acceptor states either through the formation of new states or through charge redistribution between the existing defect states.

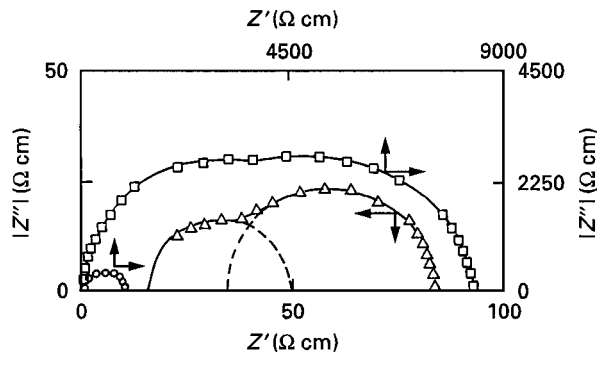

Figure 7 Complex impedance spectra of $BaTiO_3 + 0.3$ at% Nb + 3 mol% Al_2O_3 below and above T_c. (△), 300 K; (○), 423 K; (□), 450 K.

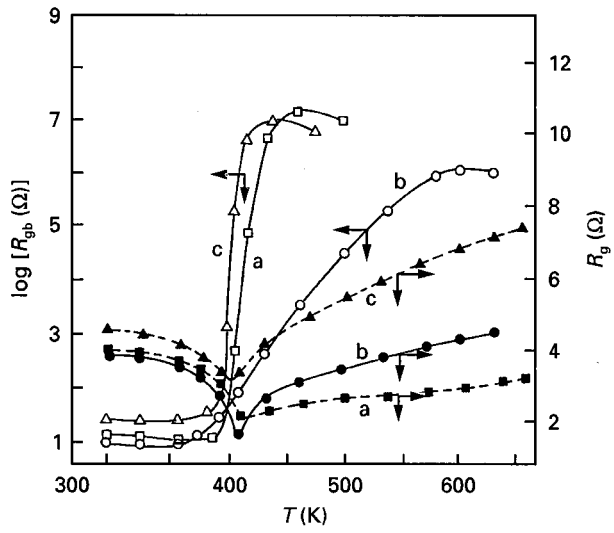

Figure 8 Variation in the grain and grain-boundary resistance with temperature for $BaTiO_3$ ceramics containing 0.3 at% Nb (curve a), 0.3 at% Nb + 3 mol% Al_2O_3 (curve b) and 0.3 at% Nb + 1 mol% B_2O_3 (curve c).

4. Discussion

Although there are various theories put forward by several workers [1, 3, 6, 7, 15, 16, 27] in explaining the PTCR in $BaTiO_3$ ceramics, all of them agree that it is caused by the trapping of charge at the grain boundaries. The debate still continues as to whether the charge carriers in n-$BaTiO_3$ are small polarons or band electrons [45, 46]. Further, the character of the electron traps were identified differently by different researchers [3, 6, 7, 13, 15, 16]. The electron traps forming the two-dimensional plane along the grain boundaries, as assumed by Heywang [1], were modified by Daniels and Wernicke [3] to include the thickness of the grain-boundary regions. From the thermodynamic equilibrium at high temperatures and the kinetic processes during cooling, they proposed a model containing a conductive grain and an insulating V''_{Ba}-rich grain-boundary zone. The V''_{Ba} act as electron traps, thereby generating the potential barrier at the grain boundaries. However, the formation of titanium vacancies can also be favoured since the formation

energy of V_{Ti} and V_{Ba} are shown to be nearly comparable [6]. The present results favour V_{Ba} in preference to V_{Ti} because of the increasing intensity of the $g = 1.997$ EPR signal with decreasing [Ba]/[Ti] ratios. Adsorbed oxygen as electron traps was suggested by Jonker [7] based on his experiments on donor-doped $BaTiO_3$ which produced PTCR jumps of three to five orders of magnitude when the specimens were annealed in an O_2 atmosphere between 800 and 1000 °C; in this temperature region, V_{Ba} diffusion from the grain boundary into the grain could be neglected. However, grain-boundary diffusion of oxygen can eliminate most of the oxygen vacancies, thereby rendering the GBL region dominant in cation vacancy compensation. Under these conditions, cation vacancy diffusion from the grain bulk is not essential for the formation of a more insulating grain-boundary region. Thus barium vacancies form the major grain-boundary electron traps in donor-doped $BaTiO_3$ although the presence of other types of electron trap, possibly at much lower densities, cannot be excluded.

Segregation of alien constituents can now bring carrier redistribution among the various charge states of barium vacancies, V^{X}_{Ba}, V'_{Ba} or V''_{Ba}, thereby affecting the electrical conductivity of the $BaTiO_3$ ceramic. The present results clearly show the drastic change in PTCR brought about by the grain-boundary modifiers such as Al_2O_3, B_2O_3 or SiO_2. This leads to the segregation of second phases such as $BaAl_6TiO_{12}$, $BaTiSi_3O_9$ or BaB_6TiO_{12}. The resulting change in PTCR can be due to the alterations in the grain-boundary structure, leading to the formation of new types of electron trap accompanied by the charge redistribution among the existing traps. The large increase in the EPR signal intensity of the $g = 1.997$ signal in the cubic and rhombohedral phases, accompanied by the large decrease in conductivity, shows that the electrons are trapped in these phases by the corresponding acceptor centres. The appearance of this signal for samples prepared without the donors and the grain-boundary modifiers followed by reduction in $H_2 + N_2$ at elevated temperatures suggests that it originates from intrinsic defect centres in $BaTiO_3$. The variation in DII with [Ba]/[Ti] ratio indicates that the associated defect centre should be the singly ionized barium vacancy, V'_{Ba}, which is EPR active. The barium vacancy, existing as neutral V^{X}_{Ba} in the tetragonal phase, converts to V'_{Ba} in the cubic phase by trapping an electron ($V^{X}_{Ba} + e' \rightleftharpoons V'_{Ba}$), thus increasing the resistivity [17, 27].

The EPR results for the specimens formulated with Al_2O_3 indicate the formation of $Al\text{–}O^-$ hole centres having axial symmetry. In the oxide lattices containing corner-shared cation polyhedra, the impurity cation with lower charges than the lattice cations can be compensated by the hole being trapped at the bridging oxygen, e.g., $Ti^{4+}\text{–}O^-\text{–}Al^{3+}$ centres in the present case. Correspondingly, the intensity of the $g = 1.997$ signal in the cubic phase decreases. This can be due to the charge redistribution among the inter-band defect states. The hole centres, having an opposite trapping character to that of electron centres, can reduce the charge occupancy of the latter and hence cause a reduction in the DII of the $g = 1.997$ signal. It has already been reported by us [33, 47] that the grain-boundary segregation of Al^{3+} as $BaAl_6TiO_{12}$ in donor-doped $BaTiO_3$ results in a higher density of trap states. The Al-related hole centres influenced by the $BaAl_6TiO_{12}$ content as well as by the grain size can, in turn, influence the charge occupancy of the trap centres present in the GBL regions. The GBLs, rich in electron traps, can be thought to be formed as the outermost layer of $BaTiO_3$ grain. It is possible that the secondary phases form an epitaxial layer over this, as supported by our SEM results. This leads to three contributions (R_g, R_{gb} and $R_{\text{secondary phase}}$) to the total resistance of the samples as is evidenced from the impedance results. A similar model of a grain-boundary phase surrounding an outer grain and the grain core has already been suggested in literature [44]. There can also be a fourth contribution from the electrode–ceramic interface.

Diffuse phase transition (DPT) behaviour (coexistence of both tetragonal and cubic phases over a range of temperatures) in donor-doped $BaTiO_3$ ceramics and its solid solutions is known in the literature [48–51], although the question as to whether its phase transformation itself is of a displacive (soft-mode) type [52–55] or of a disorder type (relaxator) [56–60] is still unresolved. Experimental evidence [52, 53, 57, 61–63] exists favouring both and, in general, a cross-over from the displacive to order–disorder behaviour can be envisaged. In semiconducting $BaTiO_3$, the order–disorder gives way to DPT behaviour. Although the origin of DPT is not very clear, it is said to be associated with the compositional [48] or thermal fluctuation [50] or with the intergranular strain distribution [64]. It is considered that the DPT in isovalent substitution is due to polarized microregions [65] with different Curie temperatures whereas, in the case of aliovalent-impurity-substituted ceramics, the formation of lattice defects additionally influence the phase transition behaviour. Donor and acceptor dopants can introduce cation or oxygen vacancies owing to the prevalence of mixed compensation [27, 66]. Such perturbations within the $BaTiO_3$ lattice not only can result in a shift in T_c but also can induce DPT behaviour due to the inhomogeneity in the spatial distribution of point defects with respect to the grain core–GBL regions. Now, an epitaxial layer of the second phase surrounding the GBL can lead to extended DPT behaviour in these ceramics and thus it is possible that the GBL can have a different T_c from the grain bulk. This can lead to a spread in energy levels of the associated GBL trap states, resulting in broad PTCR jumps.

In the case of B_2O_3 addition, the present results show that the reduction in intensity of the $g = 1.997$ signal above T_c is not accompanied by any boron-related EPR signal. This implies that B_2O_3 does not result in any new type of defect state in the GBL regions but decreases the number of activatable V'_{Ba} acceptor states. Unlike the case of Al_2O_3 addition, the ρ_{RT} is increased on B_2O_3 addition, implying the prevalence of vacancy compensation in the tetragonal phase. In that case, boron (or the glassy phase formed

through B_2O_3 addition) might influence the activation of V_{Ba}^{X} to V_{Ba}'' in the cubic phase, which are undetectable by EPR. This redistribution of charges among the point defects can lead to a decreased concentration of V_{Ba}'. Added to this, the segregated layers may not influence the diffuse nature of the GBL and hence it can have a T_c quite similar to that of the grain bulk, resulting in steeper PTCR jumps.

Thus our results show that the PTCR in $BaTiO_3$ across the tetragonal-to-cubic phase transition is exhibited through the activation of trap centres which is suitably modified by specific grain-boundary modifiers. The so-called "activation" of acceptor states which can be a result of changing vibronic characteristics of the system is evident from the fact that the activation energy for the EPR signals from the acceptor impurities is of the order of TO-phonon models [42]. Vibronic theory emphasizes the role of the electron subsystem as the origin of ferroelectric properties and was first explained on the basis of vibronic interactions (electron–lattice vibrational interactions) in perovskite-type crystals (e.g., $BaTiO_3$) by Bersuker and Vekhter [67]. The basic principle of the vibronic theory states that, under certain conditions, the mixing of the ground electronic state with nearby excited states by the dipole-type nuclear displacements (pseudo-Jahn–Teller distortion) results in the instability of the high-symmetry configuration with regard to these displacements, leading to the spontaneous polarization of the crystal. Hence the electronic band structure and the electron motion are strongly influenced by the changes in the lattice structure at the phase transition, i.e., they are dependent on the symmetry.

While the vibronic theory has been accepted for smaller-band-gap ferroelectrics, in general, the vibronic interaction concepts can also be attempted for mid-band-gap states in wide-band-gap materials such as $BaTiO_3$, particularly for the acceptor states. For the electrical transport properties, most important are the changes in localized levels in the band gap introduced by impurities as well as the native defects. Furthermore, the hole conduction is non-prevalent in the wide-band-gap materials and the acceptors are invariably self-compensated. Therefore, the concept of vibronic theory can be made use of for the defective $BaTiO_3$ containing mid-band-gap states. The energy distribution of these states is dependent on the symmetry configuration of the lattice and hence the charge redistribution at these acceptor states occurs during the structural phase transition. Barium vacancies remain neutral in the tetragonal phase whereas they are singly ionized in the cubic phase. The cation vacancies disrupt the chemical bond in $MTiO_3$ which is made up of $2p^6$ orbitals of O^{2-} ions, creating the acceptor states. During the structural phase transitions, as a result of the changing vibronic characteristics, all the V_{Ba} acceptor states are lifted out of the valence band so as to form discrete levels within the band gap and can capture electrons from the conduction band to become V_{Ba}' thus increasing the resistance. Redistribution of charges at the acceptor states arising out of the extrinsic impurities are possible by a similar mechanism. These changes are independent of the vanishing P_s and hence will account for the strong negative temperature coefficient in resistance change across the orthorhombic–rhombohedral phase transition in n-$BaTiO_3$ reported by us [68] and also the PTCR across the ferroelectric–ferroelectric transition temperature in potassium bismuth niobates [69].

It has been demonstrated through infrared [70, 71], Raman [72–74], and carrier-mobility [75–77] investigations that the charge carriers interact dominantly with the optical modes although, in general, acoustic phonons are the predominant carrier scattering modes in semiconducting materials. Detailed studies [78, 79] revealed that the electron–TO phonon interaction predominates in perovskites such as $BaTiO_3$. Indeed these TO phonons are soft in the sense that the frequency of the mode goes to zero as the T_c is approached. The major contribution to PTCR across the phase transition is expected to be due to the enhanced carrier scattering by these soft TO phonons in the vicinity of T_c. Following the electron–TO-phonon interaction model of Kobayashi *et al.* [80] to explain the resistivity anomaly of SnTe around T_c, an expression for the temperature dependence of resistivity increment across the phase transition can be obtained as

$$\Delta\rho \approx (\text{constant})\left(\frac{D_\perp}{a}\right)^2\left(\frac{k_F P_\perp}{m\Delta}\right)^2 \frac{h}{2d\omega_{TO}} N_{TO,q}(E_F)^{1/2} \tag{2}$$

Where $\Delta\rho$ is the anomalous change in resistivity across the structural phase transition, $P_\perp$ is the transverse momentum matrix element, $D_\perp$ is the transverse interband deformation potential, a is the lattice constant, d is the density of the crystal, ω_{TO} is the frequency of the TO phenon, $N_{TO,q}$ is the occupation number of the corresponding phonon and Δ is the change in energy levels between acceptor states arising owing to valency fluctuations. In the temperature regions of interest, the above equation can be further simplified by considering the approximations

$$\left(\frac{k_F P_\perp}{m\Delta}\right)^2 \approx \frac{E_F}{\Delta} \tag{3}$$

and

$$N_{TO,q} \approx \frac{kT}{h\omega_{TO}} \tag{4}$$

Hence

$$\Delta\rho \approx (\text{constant})\left(\frac{D_\perp}{a}\right)^2 \frac{E_F}{\Delta}\frac{kT}{2d\omega_{TO}^2}(E_F)^{1/2} \tag{5}$$

Thus, knowing the Δ values between the acceptor states, the change in resistivity across the phase transition could be determined. For example, $\Delta \approx 0.8$ eV between V_{Ba} and V_{Ba}' levels; $\Delta \approx 0.5$ eV between Mn^{3+} and Mn^{2+} levels in $[TiO_6]^{8-}$ octahedra as determined by the conductivity changes during optically detected magnetic resonance studies [81].

The present results show that the GBL can have a DPT and is different from the bulk owing to the

prevalence of segregated second phases such as $BaAl_6TiO_{12}$. In such a situation, Δ values can be different for the grain bulk and the GBL region, thus accounting for the broadening or steepness of PTCR curves with different grain-boundary modifiers. Good agreement between the calculated and the experimentally observed resistivity around T_c can be obtained if other multiphonon processes are also taken into consideration.

5. Conclusions

Segregation of alien constituents at the grain boundaries by way of secondary phases influences the DPT characteristics of the GBLs in donor-doped $BaTiO_3$ ceramics. This can lead to a distribution of acceptor energy levels or charge redistribution among these GBL trap states (barium vacancies being the major electron traps) which directly affect the PTCR characteristics in these ceramics. The resulting modification in PTCR (broader or steeper jumps), under such an extended DPT behaviour, can be explained on the basis of the difference between the vibronic interactions in the GBL and in the grain bulk owing to the difference in energy level separation between the trap states in these regions.

Acknowledgements

The financial support of the Department of Science and Technology, Government of India, is acknowledged by way of a project on Multifunctional Ceramic Sensors.

References

1. W. HEYWANG, *J. Mater. Sci.* **6** (1971) 1214.
2. B. HUYBRECHTS, K. ISHIZAKI and M. TAKATA, *J. Mater. Sci.* **30** (1995) 2463.
3. J. DANIELS and R. WERNICKE, *Philips Res. Rep.* **31** (1976) 544.
4. G. KOSCHEK and E. KUBALEK, *J. Amer. Ceram. Soc.* **68** (1985) 582.
5. G. KOSCHEK, *DKG* **66** (1989) 128.
6. G. V. LEWIS, C. R. A. CATLOW and R. E. W. CASSELTON, *J. Amer. Ceram. Soc.* **68** (1985) 555.
7. G. H. JONKER, *Mater. Res. Bull.* **2** (1967) 401.
8. H. IGARASHI, S. HAYAKAWA and K. OKAZAKI, *Jpn. J. Appl. Phys.* **20** (1981) 135.
9. M. KUWABARA, *Solid State Electron* **27** (1984) 929.
10. A. B. ALLES, V. R. W. AMARAKOON and V. L. BURDICK, *J. Amer. Ceram. Soc.* **72** (1989) 148.
11. T. TAKAHASHI, Y. NAKANO and N. ICHINOSE, *J. Ceram. Soc. Jpn* **98** (1990) 879.
12. H. IHRIG, *J. Amer. Ceram. Soc.* **64** (1981) 617.
13. H. UEOKA and M. YODOGAWA, *IEEE Trans. Manuf. Technol.* **3** (1974) 77.
14. H. UEOKA, *Ferroelectrics* **7** (1974) 351.
15. Y. M. CHIANG and T. TAKAGI, *J. Amer. Ceram. Soc.* **73** (1990) 3286.
16. S. B. DESU and D. A. PAYNE, *ibid.* **73** (1990) 3416.
17. T. R. N. KUTTY, P. MURUGARAJ and N. S. GAJBHIYE, *Mater. Res. Bull.* **20** (1985) 565.
18. T. R. N. KUTTY, P. MURUGARAJ, *Mater. Lett.* **3** (1985) 195.
19. P. MURUGARAJ and T. R. N. KUTTY, *J. Mater. Sci. Lett.* **5** (1986) 171.
20. Y. MATSUO, M. FUJIMURA, H. SASAKI, K. NAGASE and S. HAYAKAWA, *Ceram. Bull.* **47** (1968) 292.
21. Y. MATSUO and H. SASAKI, *J. Amer. Ceram. Soc.* **54** (1971) 471.
22. T. FUKAMI and H. TSUCHIYA, *Jpn. J. Appl. Phys.* **18** (1979) 735.
23. S. WADA and S. ATSUMI, *US Patent* 4,055,438 (1977).
24. N. FUJIKAWA and N. OTOKUMI, *Ger. Offen.* 1,941,280 (1978).
25. H. F. CHENG, *J. Appl. Phys.* **66** (1989) 1382.
26. V. RAVI and T. R. N. KUTTY, *J. Amer. Ceram. Soc.* **75** (1992) 203.
27. T. R. N. KUTTY, P. MURUGARAJ and N. S. GAJBHIYE, *Mater. Lett.* **2** (1984) 396.
28. V. RAVI and T. R. N. KUTTY, *J. Appl. Phys.* **68** (1990) 4891.
29. T. R. N. KUTTY and V. RAVI, *Appl. Phys. Lett.* **59** (1991) 2691.
30. K. KUDAKA, K. HOZUMI and K. SASAKI, *Amer. Ceram. Soc. Bull.* **61** (1982) 1236.
31. N. S. GAJBHIYE and T. R. N. KUTTY, *Bull. Electrochem. Soc.* **2** (1986) 231.
32. S. S. EATON and G. R. EATON, *Bull. Magn. Reson.* **1** (1979) 130.
33. T. R. N. KUTTY and N. S. HARI, *Mater. Lett.* **34** (1998) 43.
34. M. DROFENIK, A. POPOVIC, L. IRMANCNIK, D. KOLAR and V. KARASEVEC, *J. Amer. Ceram. Soc.* **65** (1982) C203.
35. M. DROFENIK, A. POPOVIC and D. KOLAR, *Amer. Ceram. Soc. Bull.* **63** (1984) 702.
36. N. H. CHAN and D. M. SMYTH, *J. Electrochem. Soc.* **123** (1976) 1584.
37. YU. L. DANILYUK and E. V. KHARITONOV, *Sov. Phys.—Solid State* **6** (1964) 260.
38. J. ZITKOVA, K. ZDANSKY and Z. SROUBECK, *Czech. J. Phys. B* **17** (1967) 636.
39. S. M. ARIYA, T. N. VERBITSKAYA, N. H. ENDEN and W. WINTRUFF, *J. Phys. Soc. Jpn* (Suppl.) **28** (1970) 131.
40. H. IKUSHIMA and S. HAYAKAWA, *J. Phys. Soc. Jpn* **19** (1964) 1986.
41. M. NAKAHARA and T. MURAKAMI, *J. Appl. Phys.* **45** (1974) 9.
42. T. R. N. KUTTY, L. GOMATHI DEVI and P. MURUGARAJ, *Mater. Res. Bull.* **21** (1986) 1093.
43. T. R. N. KUTTY and N. S. HARI, *Mater. Sci. Engng* **B** (1998) (accepted).
44. D. C. SINCLAIR and A. R. WEST, *J. Appl. Phys.* **66** (1989) 3850.
45. E. IGUCHI, N. KUBOTA, T. NAKAMORI, N. YAMAMOTO and K. J. LEE, *Phys. Rev. B* **43** (1991) 8646.
46. C. GILLOT, J. P. MICHENAUD, M. MAGLIONE and B. JANNOT, *Solid State Commun.* **84** (1992) 1033.
47. N. S. HARI, P. PADMINI and T. R. N. KUTTY, *J. Mater. Sci.: Mater. Elec.* **8** (1997) 15.
48. G. A. SMOLENSKY, *J. Phys. Soc. Jpn* (Suppl.) **28** (1970) 26.
49. V. I. FRITSBERG, in Proceedings of the International Meeting on Ferroelectricity, Iliffa, Prague, **1** (1966) 163.
50. A. J. BURGGRAAF and K. KEIZER, *Mater. Res. Bull.* **10** (1975) 521.
51. P. MURUGARAJ, T. R. N. KUTTY and M. SUBBARAO, *J. Mater. Sci.* **21** (1986) 3521.
52. W. G. SPITZER, R. C. MILLER, D. A. KLEINMAN and L. E. HOWARTH, *Phys. Rev.* **126** (1962) 1710.
53. J. HARADA, J. D. AXE and G. SHIRANE, *Phys. Rev. B* **4** (1971) 155.
54. H. VOGT, *J. Appl. Phys.* (Suppl. 2) **24** (1985) 112.
55. H. VOGT, J. A. SANJURJO and G. ROSSBROICH, *Phys. Rev. B* **26** (1982) 5904.
56. M. T. MASON and B. T. MATHIAS, *Phys. Rev.* **74** (1948) 1622.
57. R. COMES, M. LAMBERT and A. GUINIER, *Solid State Commun.* **6** (1968) 715.
58. A. M. QUITTET, M. LAMBERT and A. GUINIER, *Solid State Phys.* **12** (1973) 1053.

59. K. H. ESHES, H. BOCK and K. FISHER, *Ferroelectrics* **37** (1981) 507.
60. K. A. MÜLLER, W. BERLINGER, K. W. BLAZEY and J. ALBERS, *Solid State Commun.* **61** (1987) 21.
61. K. INOUE, *Jpn. J. Appl. Phys.* (Suppl. 2) **24** (1985) 107.
62. *Idem., J. Physique, Colloq. C6* **42** (1981) 430.
63. K. A. MÜLLER and W. BERLINGER, *Phys. Rev. B* **34** (1986) 6130.
64. H. T. MARTIREN and J. L. BURFOOT, *J. Phys. C* **7** (1979) 3182.
65. W. KÄNZIG and N. MAIKAFF, *Helv. Phys. Acta* **24** (1954) 343.
66. T. R. N. KUTTY and V. RAVI, *Mater. Sci. Engng* **B25** (1995) 119.
67. I. B. BERSUKER and B. G. VEKHTER, *Ferroelectrics* **19** (1978) 137.
68. T. R. N. KUTTY and N. S. HARI, *J. Phys. D* **28** (1995) 371.
69. E. I. BONDARENKO, A. N. PAVLOV, I. P. RAEVSKIL, O. I. PROKOPALD, S. M. EMELYANOV and R. F. TARASENKO, *Sov. Phys.—Solid State* **27** (1985) 1517.
70. G. LUCOVSKY, R. M. WHITE, J. A. BENDA and J. F. REVELLI, *Phys. Rev. B* 7 (1973) 3859.
71. V. V. SOBOLEV and V. I. DONESTKICH, *Phys. Stat. Sol. (b)* **45** (1971) K15.
72. R. ZALLEN and M. L. SLADE, *Phys. Rev. B* **9** (1974) 1627.
73. R. ZALLEN, *ibid. Rev.* **9** (1974) 4485.
74. K. KUMAZAKI and K. IMAI, *Phys. Stat. Sol. (b)* **149** (1988) K183.
75. A. SEGURA, F. POMER, A. CANTARERO, W. KRAUSE and A. CHEVY, *Phys. Rev. B* **29** (1984) 5708.
76. R. FIVAZ and E. MOOSER, *Phys. Rev. A* **136** (1964) 833.
77. A. SEGURA, J. P. GUESDON, J. M. BESSON and A. CHEVY, *J. Appl. Phys.* **54** (1983) 876.
78. S. H. WEMPLE, A. JAYARAMAN and M. DIDOMENICO Jr, *Phys. Rev. Lett.* **17** (1966) 142.
79. S. H. WEMPLE, M. DIDOMENICO Jr and A. JAYARAMAN, *Phys. Rev.* **180** (1969) 547.
80. K. L. I. KOBAYASHI, Y. KATO, Y. KATAYAMA and K. F. KOMATSUBARA, *Solid State Commun.* **17** (1975) 875.
81. K. MIZUSHIMA, M. TANAKA, A. ASAI, S. IDA and J. B. GOODENOUGH, *J. Phys. Chem. Solids* **14** (1979) 1129.

Received 9 June 1997
and accepted 2 April 1998